Evaluation of Free Space Optics Uplink Availability to LEO Satellite Using Climatic Data in Cairo

Adel Zaghloul[1], Abdalhameed A. Shaalan[2], H. Kasban[3], and Amal Ashraf[4]

[1] Department of Electrical Communications, Faculty of Engineering, Zagazig University, Currently at Delta University, Gamasa, Egypt

[2] Department of Electrical Communications, Faculty of Engineering, Zagazig University, Egypt

[3] Engineering Department, Nuclear Research Center, Atomic Energy Authority, Egypt

[4] Electrical and Computer Engineering department, Higher Technological Institute, Egypt

Email: adel9730101@yahoo.com; shaalan_zag2010@yahoo.com; hany_kasban@yahoo.com; aml.ashraf@hti.edu.eg

Abstract —Free space optics uplink to Low Earth Orbit (LEO) satellite with 500Km distance and 1.55μm wavelength is evaluated with 10Gbps data rate and 70W transmitted power. The equivalent effects for all weather parameters are given by the measured visibility used to determine the weather attenuations by using Mie-Scattering, in this proposed. These high attenuations reduce the availability performance of the FSO uplink. The scintillation (C_n^2) had estimated using a compatible model of Cairo weather, and the turbulence effect (beam divergence) becomes very weak by using the aperture diameter of the receiver higher than the maximum optical spot size due to turbulence and divergence. During the year 2019, the visibility must be greater than 5Km, and weak scintillation turbulence is $C_n^2 < 0.00566 * 10^{-16}$ m$^{-2/3}$ at distance 500Km. The availability evaluations based on predicted attenuation due to weather and turbulence using data measured in Cairo and the effects of all parameters on the performance of FSO are discussed. The required transmitted power must be related to the expected visibility. In year 2019, the availability of link becomes 99.9945%.

Index Terms—FSO, link availability, signal to noise ratio, egypt meteorology, scintillation, power received

I. INTRODUCTION

FSO is a line of sight (LOS) technology that depends on a narrow laser beam that transmitted information from transmitter to receiver through the atmosphere for wideband communication [1]. The precept of an FSO system operation is based on a tight optical beam that sends the modulated signal from one place to another place through the air instead of fiber optical system had used fiber cables [2]. Free space optics technology had many advantages like large data rate with high transmission security, unlicensed bandwidth spectrum, low power consumption, low bit error rates, easy deployment by saving cost [3]. The main drawback of the FSO link is channel attenuations due to various weather conditions like rain, fog, haze, snow, cloud, and even turbulence, owing to changes in temperature and pressure.

In this paper, the performance of FSO uplink to Low Earth Orbit (LEO) satellite had evaluated under tropical atmospheric conditions in Cairo for the year 2019 using λ=1550nm wavelength optical that had achieved the better availability. The block diagram of FSO uplink to satellite is shown in Fig. 1. This research focused on weather conditions and atmospheric turbulence for the performance of FSO uplink from earth to satellite, especially in tropical regions. The availability of link depends on the power received and Signal to Noise Ratio (SNR) which achieved if the value of SNR higher than the required value (SNR >15.56dB), or the value of Bit Error Rate (BER) is smaller than 10^{-9} and the power received is greater than the min value of received power. The availability of FSO link is analyzed, where it is the ratio of transmission time successfully to the transmission time failure at BER≤10^{-9}. Initiative class availability is 99.99% [4], which has outage probability about 0.01%. The class availability is higher than 99.999% in Telecommunications, while the enterprise availability ranges between 99.9% and 99.99% [5]. The availability of the link is given by:

$$\text{Av \%} = \frac{\text{successful transmission time}}{\text{total transmission time}} \qquad (1)$$

For year 2019, the availability of link becomes 99.9945%.

The paper is organized as follows. Sections II presents the related works. Section III and IV discussed the weather attenuation and atmospheric turbulence which degraded the performance of FSO link. In Section V studied FSO link performance. The results and discussions will be presented in Section VI. The conclusion is followed by Section VII.

II. RELATED WORKS

Most previous works studied the link budget analysis of horizontal FSO link under various weather conditions such as; fog and rain or haze conditions [6]. Kaushal et.al studied the scintillation and beam wander effects for FSO uplink. The results showed that, the optimum beam size depends on the fried parameter and the turbulence outer scale and it increases with by increasing the zenith angle [7].
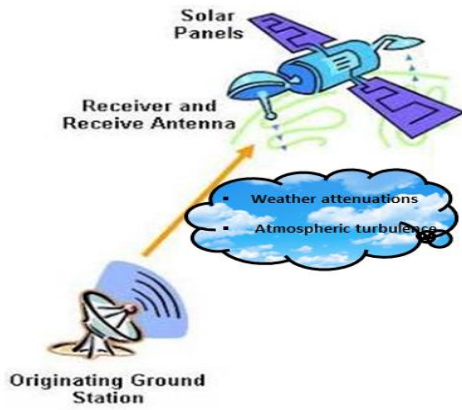
Fig. 1. Block diagram of FSO uplink.

Viswanath et.al estimated the minimum received power required for achieving the minimum BER using three modulations and spatial diversity technique scheme under different channel conditions for two links uplink and downlink [8].

K. Prabu evaluated the Performance of FSO links under strong atmospheric turbulence using different modulation schemes such as BPSK-SIM, DPSK, DPSK-SIM, PolSK and M-PPM. The results showed that, the modulation submits the finest outage probability performance and large channel capacity which achieved by formats of the DPSK scheme [9]. Mohamed H. Ibrahim studied and compared the performance of PPM, OOK, DPIM, and DH-PIM modulation schemes in FSO channels under various weather conditions. The results presented that PPM and OOK-NRZ schemes which achieved better BER performance according to the other modulations under different weather conditions [10]. Shumani estimated the availability of horizontal link of FSO using visibility data measured in orbital region over 5 km link distance in Malaysia over three years. After analysis, the link availability is 99.99% and Signal to Noise Ratio (SNR) about 37.44 dB over 1 km link distance of FSO [11].

III. Weather Attenuation

In the atmosphere, the free space optical link's quality is greatly affected by the weather conditions, such as variation of atmospheric attenuation caused by some phenomena in the atmosphere, such as scattering, absorption, and turbulence [12]. Scattering, which is produced by fog, rain, haze, or low clouds, leads to attenuating the information signal before receiving it at the receiver and limiting the availability of the FSO system [13], [14].

A. Scattering Attenuation

One of the major effects of the weather condition is caused by fog as it leads to absorption and scattering. The atmospheric visibility had measured to predict the atmospheric environmental conditions. The visibility known as the maximum distance propagated using 550nm optical wavelength where, its disparity drops to fraction

roughly 2% or 5% of original signal power. Atmospheric attenuation owing to fog can be predicted by applying Mie scattering theorem that determines the scattering attenuation coefficient [15], [16] which based on meteorological data using the empirical models as [17], [18]:

$$\beta = \frac{3.912}{V}\left[\frac{550nm}{\lambda}\right]^{\delta}(Km) \qquad (2)$$

Both Kruse and Kim model could be used to predict the attenuation using visibility in dB/km [17] is given by the equation [18]:

$$\alpha_{sct} = \frac{-10logV\%}{V(Km)} * \left(\frac{550}{\lambda}\right)^{\delta}(dB/Km) \qquad (3)$$

where, V% is the percentage transmission of air drops for clear sky and -10log V% equals to 17/V and 13/V for 2% and 5% visibility distance respectively [19], V is the visibility in Km, λ stands for operating wavelength in (nm), and δ stands for the size distribution coefficient of scattering which depends on visibility ranges is given by:

- For Kruse model [20]

$$\delta = \begin{cases} 1.6 & for & V > 50Km \\ 1.3 & for & 6 < V < 50Km \\ 0.585\,V^{(1/3)} & for & V < 6Km \end{cases} \qquad (4)$$

- For Kim model [21]

$$\delta = \begin{cases} 1.6 & for\ V > 50Km \\ 1.3 & for\ 6Km < V > 50Km \\ 0.16\,V + 0.34 & for\ 1Km < V > 6Km \\ V + 0.5 & for\ 0.5Km < V > 1Km \\ 0 & for\ V < 0.5Km \end{cases} \qquad (5)$$

Also, Al Naboulsi model had used to expect specific attenuation by using wavelength. It had produced relations to predict the attenuation of convection fog and advection fog separately. The advection fog produced by moving warm and wet air masses forms which are considered by the liquid water content above 0.20 g/m^3 and a particle diameter around to 20 μm [22]. The attenuation coefficient for the advection fog attenuation is given by:

$$\rho_{adv}(\lambda) = \frac{0.11478\,\lambda + 3.8367}{V(Km)} \qquad (6)$$

Radiation fog occurs at night of the day when the air is iced by radiation and becoming saturated. The liquid water ranges from 0.01 to 0.1 g/m3, and the particle diameter is about 4μm. The attenuation coefficient for the radiation fog attenuation is given by:

$$\rho_{rad}(\lambda) = \frac{0.18126\,\lambda^2 + 0.13709\,\lambda + 3.7205}{V(Km)} \qquad (7)$$

The specific attenuation for both advection and radiation fog in (dB/km) [23] is given by:

$$\alpha_{sct} = 4.34\,\{\rho(\lambda)\} = \frac{10}{\ln 10}\{\rho(\lambda)\}(dB/Km) \qquad (8)$$

B. Cloud Attenuation

Cloud attenuation had categorized based on cloud number concentration (N_c) [24], height, liquid water contents (LWC), and water droplet size. The data for LWC calculated from the vertical atmospheric profile into satellite, which had estimated the visibility range through clouds by dividing the vertical atmosphere into cloud layers [19]. Each layer has a value of the LWC, and cloud number concentration summaries with height used to get the visibility estimate. The corresponding visibility is expressed as [25]:

$$V = 1.002/(LWC * N_c)^{0.6473} \qquad (9)$$

Then, the cloud attenuations are like fog attenuations measurement using the visibility range estimate, L_{cloud} is expressed as:

$$L_{cloud} = 4.34 * \alpha_{sct} * d \qquad (10)$$

The coefficients of attenuation and visibility for the different types of cloud are taken from [26].

C. Rain Attenuation

The Rain attenuation had produced by non-selective scattering since the raindrop radius (200-2000μm) is greater than the wavelength of the light source of FSO system [6]. The attenuation of rain is one of the weather attenuation effects on the reliability of FSO system. The attenuation of rain which measured in (dB/Km) is given by [27].

$$\alpha_{rain} = k\, R_{rain}^{a}\,(dB/Km) \qquad (11)$$

where, R_{rain} stands to the rain intensity in (mm/hr), K and a are rain coefficients [28] which depend on carrier wavelength of the FSO system. The values of these coefficients K and a can be obtained from model in [29] which developed for FSO in tropical climate. Then the values of k and a are obtained as 1.076 and 0.67 respectively for Carbonneau model.

D. Snow Attenuation

Snow attenuation is one of the weather attenuations which less than fog attenuation but more than rain attenuation. During heavy snow, the laser beam path had blocked because of increasing the density of snowflakes in the propagation path or owing to the configuration of ice on window pane [30]. This attenuation had reduced the link availability of the FSO system. The snow attenuation has been organized into dry and wet snow attenuation. The specific attenuation for snow in (dB/Km) is given by:

$$\alpha_{snow} = a\, S^{b} \qquad (12)$$

where, S stands to the snow rate in (mm/hr) and the values of parameters a and b in dry and wet snow is given:

- For dry snow:

$a = 5.42 * 10^{-5} + 5.49, \qquad b = 1.38$

- For wet snow:

$a = 1.02 * 10^{-4} + 3.78, \qquad b = 0.72$

IV. TURBULENCE AND BEAM WANDER EFFECTS

A. Atmospheric Turbulence (Scintillation)

Atmospheric turbulences are generated because of changes in temperature and pressure for airflow. It had considered one of the most important challenges in the FSO systems. The propagated optical signal through space was affected by the atmospheric turbulence caused by the changing of the air temperature or the pressure and Relative Humidity (RH) [31]. These changes produced variations in the refractive index of the medium [32], [33] which changes randomly with space and time. The refraction index fluctuation produced a deflection of the optical beam and then variations of power received at the receiver end. Atmospheric turbulence due to fluctuation in air mass is modeled by gamma-gamma distributed channel and expressed as [34], [35];

$$F_h(h) = \frac{2(\alpha\beta)^{\frac{\alpha+\beta}{2}}}{\Gamma(\alpha)\Gamma(\beta)}\, h^{\left(\frac{\alpha+\beta-1}{2}\right)}\, K_{\alpha-\beta}\left(2\sqrt{\alpha\beta h}\right) \quad (13)$$

where, α and β are the values of spherical wave [36], the distribution shaping parameter $K_{\alpha\text{-}\beta}(\cdot)$ represents the modified second order Bessel function, $\Gamma(\cdot)$ denotes the gamma function. α and β can be defined as,

$$\alpha = \left\{ \exp\left[\frac{0.49\sigma_R{}^2}{(1+0.56\sigma_R{}^{12/5})^{7/6}} \right] - 1 \right\}^{-1}$$

$$\beta = \left\{ \exp\left[\frac{0.51\,\sigma_R{}^2}{(1+0.69\,\sigma_R{}^{12/5})^{5/6}} \right] - 1 \right\}^{-1}$$

where, $\sigma_R{}^2 = 1.23\, C_n^2\, K^{7/6}\, L^{11/6}$ represents the Rytov variance of spherical wave [37], C_n^2 is the refractive index of turbulence, $K = 2\pi/\lambda$ is the optical wave number [34], and λ is the operating wavelength. L is the link length.

B. Beam Wander or Spreading

Turbulence Effects on the spot sizes called spreading. When the in homogeneities are less than the size of beam diameter, they tend to broaden the beam, but do not deflect it [5]. This is called beam spreading which shown in Fig. 2. It defocuses the beam reducing its intensity.

The beam will experience a degradation in quality so that the average beam waist in time will be $W_{eff} > W_{rec}$. The beam spreading can be described using the effective beam waist average as [38]:

$$W_{eff} = W_{rec}\left\{ 1 + 1.33\sigma^2 \left(\frac{2\,L}{K * W_{rec}} \right)^{5/6} \right\}^{1/2} \quad (14)$$
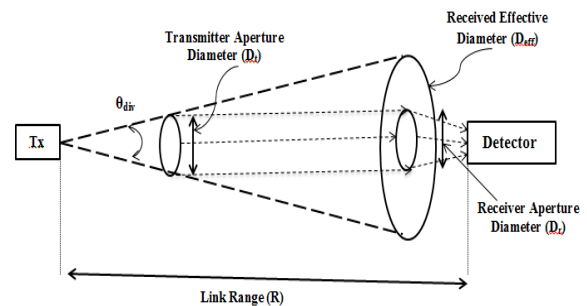

Fig. 2. Beam divergence losses.

where W_{rec} is the waist beam (diameter of receiver D_{rec}) at propagation distance L in (Km) which expressed as [39]:

$$W_{rec} = W_o + \theta_{div} L \qquad (15)$$

where W_o stands to initial beam waist that transmitter aperture diameter D_t in (cm), the divergence angle is $\theta_{div} = \lambda / 10 \Pi \, D_t$ in (mrad), λ wavelength in (μm). The geometric loss (beam divergence loss) in dB will be [19]:

$$\alpha_{Geo}(dB) = 20 \, log\left(\frac{W_{eff}}{W_{rec}}\right) \qquad (16)$$

α_{Geo} is ignored with $D_{rec} > D_{eff}$

Also, the beam wander had decreased by using the receiver aperture diameter (D_{rec} more than the effective beam waist (received effective diameter D_{eff}). In proposed system diameter of transmitter $D_t = 10$ cm, from equation diameter of receiver $D_{rec} = 256.69$ cm = 2.5669 m, calculating D_{eff} from its equation as: $D_{eff} = 267.5$cm = 2.675m, the ratio of

$$\frac{D_{eff}}{D_r} = \frac{267.5}{256.69} = 1.04$$

The receiver aperture diameter becomes:

$$D_r = 1.04 \, D_{eff} = 278.765 cm = 2.78765 m$$

The telescope aperture diameter is available at 10m, this research take D_{rec} =3 m, so, the geometric losses are ignored.

V. FSO Link Performance Evaluation

A. Power Received

In terms of power received, the receiver sensitivity determined the amount of optical power received which is required to evaluate the required SNR is greater than 15.56 dB and Bit Error Rate less than 10^{-9} for a given estimated FSO communication performance. The expression of signal power received at the communications detector for FSO communication link P_{rec} is expressed as [40], [41]:

$$P_{rec} = P_T \, G_T \, G_{rec} L_{free \, space}^{-1} \tau_T \tau_{rec} \alpha_{Geo} 10^{-0.1\alpha_{atm} L} \, (17)$$

where, P_T stands for optical transmitted power (W), $G_T = (\pi D_t/\lambda)^2$ [42], [43] stands the transmitter gain, $G_{rec} = (\pi D_{rec}/\lambda)^2$ stands the receiver gain and D_t and D_{rec} are the diameter of transmitter and receiver respectively in (cm), λ is the wavelength in (μm), τ_T and τ_{rec} are the transmitter and receiver optical efficiencies, α_{atm} is the value of the atmospheric transmission attenuations in (dB/Km), L is the length between the ground station and LEO satellite in (Km). L $_{free \, space}$ is the free space loss which is the major factor degraded the optical signal received [44]. The signal transmitted from the ground station to LEO satellite through free space is reduced. The free space loss is expressed as:

$$L_{free \, space} = (\lambda/4\pi L)^2 \qquad (18)$$

The value of power received P_{rec} should be more than the sensitivity of the optical detector (P_{rmin} = -43dBm) and less than the maximum power received (P $_{rmax}$ = -13dBm).

$$P_{rec} = 6.1685 * 10^{-3} P_T \frac{D_t^2 D_{rec}^2}{\lambda^2 L^2} 10^{-0.1\alpha_{atm} L} \quad (19)$$

In the proposed design, the received power becomes:

$$P_{rec} = 0.0924 * 10^{-50 \, \alpha_{atm}} P_T \qquad (20)$$

At great weather attenuation, the optical power received will be reduced so, we need the heavy value of transmitted power P_T. Also, the received power required to achieve a BER less than 10^{-9} at a given data rate. The required power is defined as [45]:

$$P_{required} = E_p \, \eta N_p \, R \qquad (21)$$

where, E_p=hc/λ is the photon energy, h= 6.625* 10^{-34} J.s stands the blank's constant, the speed of light in air is c = $3*10^8$ m/s, η is the quantum efficiency of the receiver, N_p is the receiver sensitivity (photons/bits), and R is the data rate (Gbps), the received power becomes:

$$P_{rec} = 1.9875 * 10^{-10} \frac{\eta \, N_p \, R}{\lambda} \qquad (22)$$

B. SNR and BER

The two major evaluation parameters for FSO system are SNR and BER [46], [47]. The optical signal had converted into electrical signal by photodetector devices at the receiver. The almost photodetector used in optical communication systems is PIN photodetector because it has suitable material, high sensitivity, fast response time, and small size [40]. SNR is the ratio of signal power to noise power given by [48]:

$$SNR = \eta \, N_p \qquad (23)$$

Therefore, from the above equations of power received, the SNR becomes,

$$SNR = 31.036477 * 10^6 \frac{D_t^2 D_{rec}^2}{\lambda L^2} 10^{-0.1\alpha_{atm} L} \left(\frac{P_T}{R}\right) \quad (24)$$

From proposed design, D_{rec} =300cm, and D_t =10cm, the SNR well get from

$$SNR = 7.2 * 10^8 * 10^{-50 \, \alpha_{atm}} \left(\frac{P_T}{R}\right) \qquad (25)$$

With P_T = 70w = 48.45dBm, and R = 10Gbps, the SNR becomes:

$$SNR = 50.4 * 10^8 * 10^{-50 \, \alpha_{atm}} \qquad (26)$$

Then, the max suitable weather attenuation α_{atm} is 0.16 dB/Km for Signal to Noise Ratio is 15.56 dB and the min suitable visibility is 4.446Km.

Bit Error Rate of 10^{-6} agrees to on average one error per million bits. Perfectly, the value of BER must be 10^{-9} as the maximum error rate existent in the receiving of bits for a reliable and long distance communication system [49], [50].

$$BER = \frac{No.\,of\,Errors}{Total\;No.\,of\,bits} \qquad (27)$$

The relationship between BER and SNR or Q factor had described in equation (22) for NRZ-OOK coded optical data and detected with a PIN photodiode. The Q-factor value is greater than required value of 7.

$$BER_{NRZ-OOK} = \frac{1}{2}erfc\left(\frac{1}{2\sqrt{2}}\sqrt{SNR}\right) = \frac{1}{2}erfc\left(\frac{Q}{\sqrt{2}}\right) \;(28)$$

VI. RESULTS AND DISCUSSIONS

The proposed design in this research for FSO uplink to LEO satellite with optical wavelength λ=1550nm, link range is 500Km, power transmitted P_T=70W =48.45dBm, divergence angle θ_{div} = 0.00493mrad, and data rate R=10Gbps using climatic data in Cairo through year 2019. Therefore, this paper aims to predict the availability of FSO performing link from earth to satellite, especially LEO satellite, by analyzing attenuations that had degraded the link under tropical atmospheric conditions.

The computations of weather attenuations and atmospheric turbulence effects are based on meteorological data measured in Cairo. Scintillation evaluated C_n^2 (m$^{-2/3}$)

$$C_n^2 = 10^{-16} * TWP$$

where, TWP is the turbulence weather parameter given by:

$$TWP = -5300 + 20T + 380W_{th} +$$
$$\{-28RH + 0.29RH^2 - 0.0011RH^3\} +$$
$$\{-25W_s + 12W_s^2 - 0.85W_s^3\}$$

where T is the temperature in (°K), W_{th} is the temporal-hour weight is defined from Table I based on the value of C_{th}, RH stands to the relative humidity in (%), W_s stands to the wind speed in (m/s).

$$C_{th} = \frac{12 * (current\,hour - sunrise\,hour)}{(sunset\,hour - sunrise\,hour)}$$

*Calculating of the scintillation over one day in 2019, for example 20 January 2019.

In this date, sunrise at 6:50, sunset at17:21 and midday at 12.00

- At current hour = 7:0 (near sunrise),
  $T = 9°C = 9 + 273 = 282°K$, $RH = 87\%$,
  $W_s = 9Km/h = 2.5m/s$. So,
  $$C_{th} = \frac{12\{(7*60-0)-(6*60+50)\}}{(17*60+21)-(6*60+50)} = 0.1907$$

From table (I), W_{th} =0.05,

$$TWP = -607, C_n^2 = -607 * 10^{-16}m^{-2/3}$$

- At current hour = 12:0 (midday),

$T = 290°K, RH = 49\%, W_s = 5.278\ m/s$. So,

$$C_{th} = \frac{12\{(12*60-0)-(6*60+50)\}}{(17*60+21)-(6*60+50)} = 5.89 ,$$

From Table I

$$W_{th} = 1TWP = 152 , C_n^2 = 152 * 10^{-16}m^{-2/3}.$$

- At current hour = 18:0 (near sunset),

$T = 289°K, RH = 63\%, W_s = 3.6m/s$. So,

$$C_{th} = \frac{12\{(18*60-0)-(6*60+50)\}}{(17*60+21)-(6*60+50)} = 12.7$$

From table (I)

$$W_{th} = 0.1, TWP = -344, C_n^2 = -344 * 10^{-16}m^{-2/3}.$$

TABLE I: THE VALUE OF TEMPORAL-HOUR WEIGHT W_{TH} CORRESPONDING TO C_{TH}

event	night	night	Night	night	Night
C_{th}	until -4	-4 to -3	-3 to -2	-2 to -1	-1 to 0
W_{th}	0.11	0.11	0.07	0.08	0.06
event	day	day	Day	day	Day
C_{th}	5-6	6-7	7-8	8-9	9-10
W_{th}	1.0	0.90	0.80	0.59	0.32
event	sunrise	day	Day	day	Day
C_{th}	0-1	1-2	2-3	3-4	4-5
W_{th}	0.05	0.10	0.51	0.75	0.95
event	day	sunset	Night	night	Night
C_{th}	10-11	11-12	12-13	Over 13	
W_{th}	0.22	0.1	0.08	0.13	

The value of C_n^2 at midday is higher than the values at sunrise and sunset. So, take weather data at midday for all days of year 2019. This paper estimated C_n^2 values at midday. Calculations of scintillation index (σ^2) at midday through year 2019 in Egypt, Scintillation index for week turbulence is less than one for plain wave ($\sigma^2 \leq 1$) from equation (16) is given by:

$$\sigma^2 = 1.23 * 10^{-16} TWP\left(\frac{2\pi}{\lambda}\right)^{7/6} L^{11/6}$$

With λ in μm, and L in Km;

$$\sigma^2_{week} = 3.3198 * 10^{-3} TWP\left(\frac{1}{\lambda}\right)^{7/6} L^{11/6}$$

For this design, L=500Km, and λ =1.55μm, the value of $\sigma^2 = 176.673\ TWP$, and the maximum allowable week scintillation index σ^2 =1 which occurs at:

$C_n^2 = 0.00566 * 10^{-16}\ m^{-2/3}$.

The maximum value of distance increases while decreasing TWP turbulence with σ^2 week < 1, and λ = 1.55 μm, the max distance must be:

$$3.3198 * 10^{-3} TWP\left(\frac{1}{1.55}\right)^{7/6} (L_{max})^{11/6} < 1$$

$$L_{max} < \left(\frac{1}{1.9909 * 10^{-3}TWP}\right)^{6/11}$$

$$< 29.7335 \ (TWP)^{-6/11}$$

The values of σ^2 at midday for all days of year 2019 are shown in Fig. 3. The condition of scintillation index which has $\sigma^2 \le 1$ is achieved for all days except, on 25 February, 1, 12, 13, 14, 15, 16, 21, 22, 23 May, 17July, and 15 August 2019, the values of scintillation index (σ^2) are 1.022, 1.025, 1.0175, 1.0753, 1.099, 1.0057, 1.1057, 1.0815, 1.159, 1.189, 1.081, and 1.095 respectively. And the maximum lengths that allowed at these dates are 488Km, 486.5Km, 490.6Km, 461.9Km, 451.01Km,

496.9Km, 448.075 Km, 459Km, 425.5Km, 413.79Km, 413.79Km, 459.25Km, and 452.863Km respectively.

For proposed design, the PIN detector receiver which has quantum efficiency (η=0.9), bandwidth = data rate/2 =5GHz, and sensitivity (P_{rmin} = 50nW= -43dBm, P_{rmax} =50μW = -13 dBm). The power received values P_{rec} in (dBm) at midday for all days of year 2019 are shown in Fig. 4. The condition of received power which has P_{rec} is greater than P_{rmin} which equals -43 dBm ($P_{rec} \ge P_{rmin}$) is achieved for all days except, at 13 February 2019 which equals -31.96dBm.
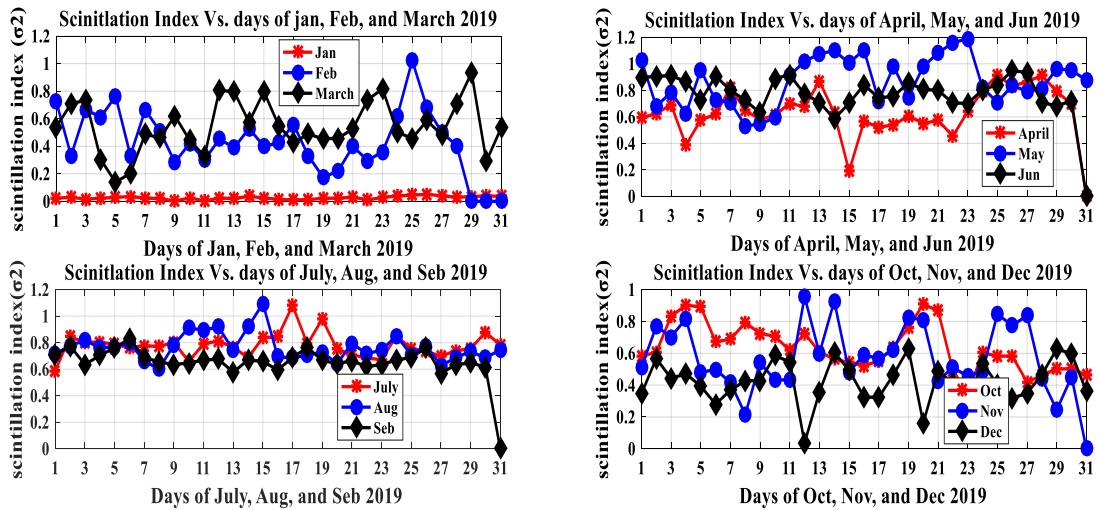

Fig. 3. Scintillation index ($\sigma2$) Vs. all days of year 2019.
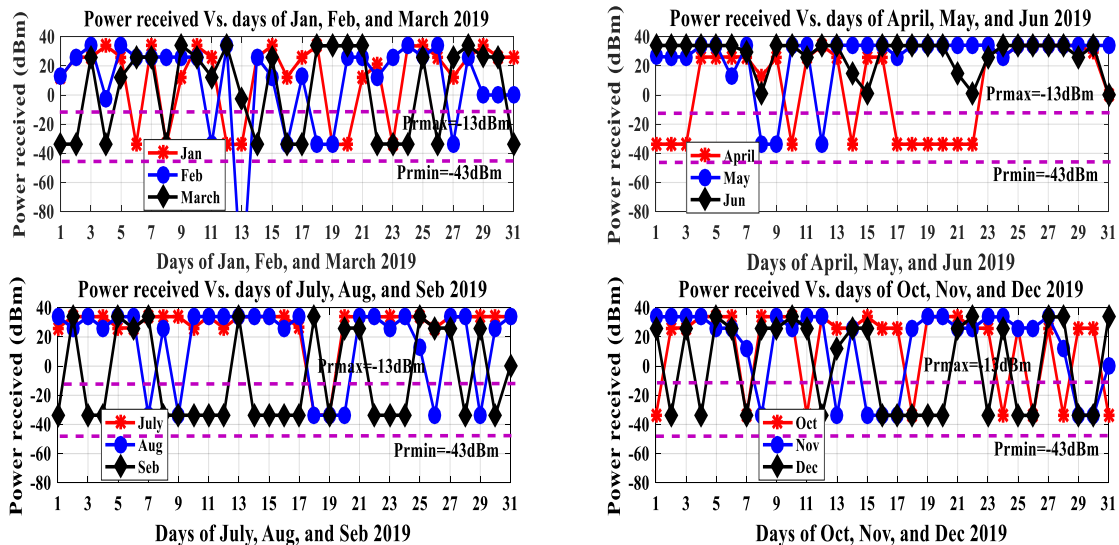

Fig. 4. Power received Vs. all days of year 2019.

The SNR values at midday for all days of year 2019 are shown in Fig. 5. The condition of SNR is greater than or equals 15.56 dB (SNR $\ge$ 15.56dB) which achieved for all days of year 2019 except, at 13 Feb 2019, the value of SNR is equal to -73.049dB.

VII. CONCLUSION

Free Space Optics is a growing technology that presents high data rates that is suitable for wireless communications. This paper has evaluated the availability

performance of FSO system uplink from earth to LEO satellite in the tropical region in Cairo through the year 2019 by analyzing all attenuations that degraded the performance link. FSO system is affected by atmospheric attenuation and turbulence. These high attenuations reduce the availability performance of the FSO uplink. The proposed system was evaluated with distance 500Km, wavelength λ=1.55μm, and data rate =10Gbps using NRZ-OOK, PIN photodiode. The availability evaluations are based on predicted attenuation due to weather and turbulence using data measured in Cairo. This link's performance is characterized by received optical power, SNR higher than 15.56dB, and BER less than 10-9. In

this paper, the availability assessment of FSO has been evaluated for atmospheric conditions and turbulence. During analysis, the availability of the link becomes 99.9945%. The optimum Signal to Noise Ratio and minimum Bit Error Rate for FSO uplink depends upon the transmitted power and data rate. Increase the SNR while increasing the transmitted power and decreasing the data rate. The required transmitted power must be related to the expected visibility. The performance of this link was achieved for all days of the year 2019, except one day. This paper will be a useful tool for vertical FSO link, especially under tropical climate conditions.
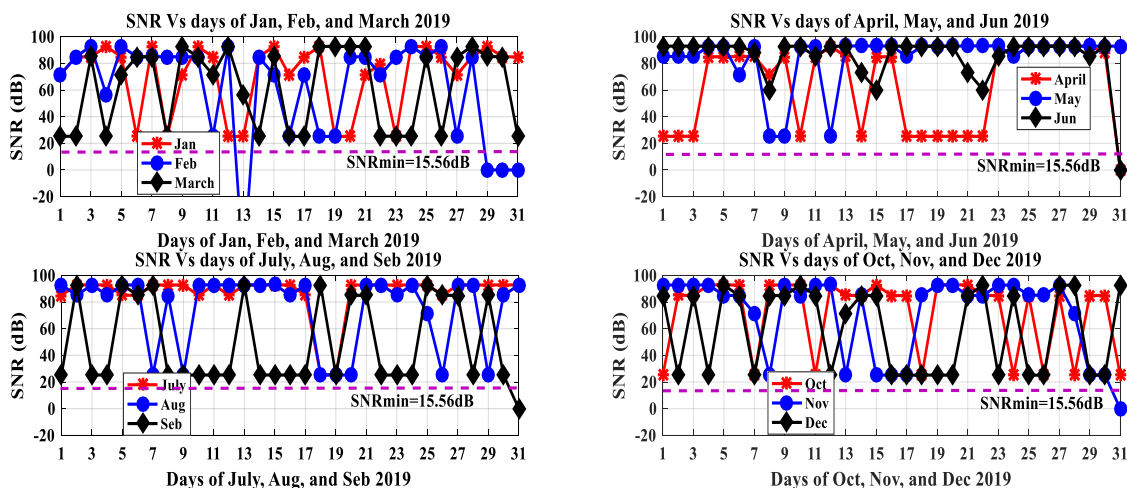

Fig. 5. Signal to noise ratio Vs. all days of year 2019

CONFLICT OF INTEREST

There is no conflict of interest.

This manuscript has not been submitted to, nor is under review at, another journal or other publishing vanue.

The authors have no affiliation with any organization with a direct or indirect financial interest in the subject matter discussed in the manuscript.

AUTHOR CONTRIBUTIONS

Adel Zaghloul: Conceptualization, Methodology, Software Validation, Original draft preparation, Writing- Reviewing and Editing.

Abdalhameed A. Shaalan: Conceptualization, Methodology, Software Validation, Original draft preparation, Writing- Reviewing and Editing.

H. Kasban: Conceptualization, Methodology, Software Validation, Original draft preparation, Writing- Reviewing and Editing.

Amal Ashraf: Conceptualization, Methodology, Software Validation, Original draft preparation, Writing- Reviewing and Editing.

REFERENCES

[1] S. A. Al-Gailani, A. B. Mohammad, M. S. Islam, U. U. Sheikh, and R. Q. Shaddad, "Tropical temperature and humidity modeling for free space optical link," *Journal of Optics*, vol. 45, pp. 87–91, 2016.

[2] S. A. Al-Gailani, A. Mohammad, U. U. Sheikh, and R. Q. Shaddad, "Determination of rain attenuation parameters for free space optical link in tropical rain," *Optik*, vol. 125, pp. 1575-1578, 2014.

[3] A. Basahel, I. M. Rafiqul, M. H. Habaebi, and A. Z. Suriza, "Visibility effect on the availability of a terrestrial free space optics link under a tropical climate," *Journal of Atmospheric and Solar-Terrestrial Physics*, vol. 143, pp. 47–52, 2016.

[4] M. Ali and A. Ali, "Performance analysis of fog effect on free space optical communication system," *IOSR J. Appl. Phys*, vol. 7, no. 2, pp. 16–24, 2015.

[5] S. A. Zabidi, R. Islam, and W. F. Al-Khateeb, "Analysis of free space optics link availability with real data measurement in tropical weather," in *Proc. International Conference Computer and Communication Engineering (ICCCE)*, 2014, pp. 197–200.

[6] D. Kakati and S. C. Arya, "Performance of 120 Gbps single channel coherent DP-16-QAM in terrestrial FSO link under different weather conditions," *Optik*, vol. 178, pp. 1230-1239, 2019.

[7] H. Kaushal, G. Kaddoum, V. K. Jain, and S. Kar, "Experimental investigation of optimum beam size for FSO uplink," *Optics Communications*, vol. 400, pp. 106–114, 2017.

[8] A. Viswanath, V. K. Jain, and S. Kar, "Reduction in transmitter power requirement for earth to-satellite and satellite-to-earth free space optical links with spatial diversity," *Opt. Quant Electron*, vol. 418, 2018.

[9] K. Prabua, D. S. Kumara, and T. Srinivas, "Performance analysis of FSO links under strong atmospheric turbulence conditions using various modulation schemes," *Optik*, Vol. 125, pp. 5573–5581, 2014.

[10] M. H. Ibrahim, H. A. Shaban, and M. H. Aly, "Effect of different weather conditions on BER performance of single-channel free space optical links," *Optik*, vol. 137, pp. 291–297, 2017.

[11] M. M. Shumania, M. F. L. Abdullaha, and A. Basahel, "Availability analysis of terrestrial Free Space Optical (FSO) link using visibility data measured in tropical region," *Optik*, vol. 158, pp. 105–111, 2018.

[12] S. Malik and P. K. Sahu, "Free space optics/millimeter-wave based vertical and horizontal terrestrial backhaul network for 5G," *Optics Communications*, vol. 459, 2020.

[13] T. S. Hanzr and G. Singh, "Performance of free space optical communication system with BPSK and QPSK Modulation," *IOSR Journal of Electronics and Communication Engineering*, vol. 1, no. 3, pp. 38-43, 2012.

[14] T. S. Hanzr and G. Singh, "Improvement in performance of free space optical communication," *International Journal of Applied Information Systems*, vol. 2, no. 4, 2012.

[15] M. Ijaz, Z. Ghassemlooy, J. Pesek, O. Fiser, H. L. Minh, and E. Bentley, "Modeling of fog and smoke attenuation in free spaceoptical communications link under controlled laboratory conditions," *Journal of Light wave Technol*, vol. 31, no.11, pp. 1720–1726, 2013.

[16] S. M. Rajendrakumar and M. Karruppaswamy, "Analysis of link availability in FSO-OFDM system under various climatic conditions," *Engineering Journal*, vol. 19, no. 1, 2015.

[17] A. Basahel, I. M. Rafiqul, A. Z. Suriza, and M. H. Habaebi, "Availability analysis of free-space-optical links based on rain rate and visibility statistics from tropical a climate," *Optik-International Journal Light Electron Optics*, vol. 127, no. 22, pp. 10316-10321, 2016.

[18] A. Ashraf, A. Zaghloul, A. A. Shaalan, and H. Kasban, "Effect of fog and scintillation on performance of vertical free space optical link from earth to LEO satellite," *International Journal of Satellite Communications and Networking*, vol. 39, no. 3, 2021.

[19] M. Alzenad, M. Z. Shakir, H. Yanikomeroglu, and M. S. Alouini, "FSO-based vertical backhaul/fronthaul framework for 5G+ wireless networks," *IEEE Communications Magazine*, vol. 56, no. 1, pp. 218–224, 2018.

[20] H. Kaushal, V. K. Jain, and S. Kar, "Free space optical communication, optical networks," Book Chapter, Free-Space Optical Channel Models, Springer (India) Pvt. Ltd., 2017.

[21] M. Grabner and V. Kvicera, "Fog attenuation dependence on atmospheric visibility at two wavelengths for FSO link planning," in *Proc. IEEE Antennas and Propagation Conference*, Loughborough, England, 2010, pp. 193–196.

[22] M. A. Naboulsi, H. Sizun, and F. D. Fornel, "Fog attenuation prediction for optical and infrared waves," *Optical Engineering*, vol. 43, pp. 319-329, 2004.

[23] M. Ali and A. Ali, "FSO communication characteristics under fog weather condition," *International Journal of Scientific & Engineering Research*, vol. 6, no. 1, 2015.

[24] A. Viswanath, V. K. Jain, and S. Kar, "Aperture averaging and receiver diversity for FSO downlink in presence of atmospheric turbulence and weather conditions for OOK, MPPM and M-DPPM schemes," *Optical and Quantum Electronics*, vol. 9, 2016.

[25] A. Viswanath, V. Kumar, and S. Kar, "Analysis of earth-to-satellite free-space optical link performance in the presence of turbulence, beam-wander induced pointing error and weather conditions for different intensity modulation schemes," *IET Communications*, vol. 9, no. 18, pp. 2253–2258, 2015.

[26] M. S. Awan, Marzuki, E. Leitgeb, B. Hillbrand, F. Nadeem, and M. S. Khan, "Cloud attenuations for free-space optical links," in *Proc. International Workshop on Satellite and Space Communication*, 2009, pp. 274-278.

[27] A. Z. Suriza, A. K. Wajdi, I. M. Rafiqul and A. W. Naji, "Preliminary analysis on the effect of rain attenuation on free space optics (FSO) propagation measured in tropical weather condition," in *Proc. International Conference on Space Science and Communication*, 2011, pp. 96-101.

[28] M. Ali and A. Ali, "Analysis study of rain attenuation on optical communications link," *International Journal of Engineering, Business and Enterprise Applications*, vol. 6, pp. 18-24, 2013.

[29] S. A. Zabidi, I. M. Rafiqul, and A. K. Wajdi, "Rain attenuation prediction of optical wireless system in tropical region," in *Proc. International Conference Smart Instrumentation, Measurement and Applications (ICSIMA)*, 2013, pp. 1–5.

[30] H. Kaushal and G. Kaddoum, "Optical communication in space: Challenges and mitigation techniques," *IEEE Communications Surveys & Tutorials*, vol. 19, no. 1, pp. 57-96, 2017.

[31] M. K. El-Nayal, M. M. Aly, H. A. Fayed, and R. A. AbdelRassoul, "Adaptive free space optic system based on visibility detector to overcome atmospheric attenuation," *Results in Physics*, vol. 14, 2019.

[32] T. Ismail, E. Leitgeb, Z. Ghassemlooy, and M. Al-Nahhal. "Performance improvement of FSO system using multi-pulse pulse position modulation and SIMO under atmospheric turbulence conditions and with pointing errors," *IET Networks*, vol.7, no. 4, pp. 165-172, 2018.

[33] L. Andrews, R. Phillips, and C. Hopen, *Laser Beam Scintillation with Applications*, Washington: Spie Press, 2001.

[34] F. A. Mahdavi and H. Samimi, "Performance analysis of MIMO-FSO communication systems in gamma-gamma turbulence channels with pointing errors," in *Proc. 24th Iranian Conference on Electrical Engineering (ICEE)*, 2016, pp. 822-827.

[35] P. Kaur, V. K. Jain, and S. Kar, "Performance analysis of FSO array receivers in presence of atmospheric turbulence," *IEEE Photonics Technology Letters*., vol. 26, no. 12, pp. 1165-1168, 2014.

[36] H. Kashif, M. N. Khan, and A. Altalbe, "Hybrid optical-radio transmission system link quality: Link budget analysis," *IEEE Access*, 2020.

[37] H. Kashif, M. N. Khan, and A. Rafay, "Performance and optimization of hybrid FSO/RF communication system in varying weather," *Photonic Network Communications*, 2020.

[38] J. Recolons, L. C. Andrews, and R. L. Phillips, "Analysis of beam wander effects for a horizontal-path propagating Gaussian-beam wave: focused beam case," *Optical Engineering*, vol. 46, no. 8, pp. 1-12, 2007.

[39] A. N. Z. Rashed, A. A. Mohammed, and E. S. El-Dien, "Free space and under water optical wireless communication systems evaluation," *International Journal of Review in Electronics & Communication Engineering*, vol. 2, no. 5, pp. 145-160, Oct. 2014.

[40] M. A. Ali and E. H. Ahmed, "Performance of FSO communication system under various weather condition," *Advances in Physics Theories and Applications*, vol. 43, pp. 10-18, 2015.

[41] K. R. Ummul, M. S. Anuar, A. K. Rahman, C. B. M. Rashidi, and S. A. Aljunid, "The performance in FSO communication due to atmospheric turbulence via utilizing new dual diffuser modulation approach," *International Journal of Applied Engineering Research*, vol. 12, no. 7, pp. 1416-1420, 2017.

[42] A. Akbulut, H. AlparslanIlgin, and M. Efe, "Adaptive bit rate video streaming through an RF/free space optical laser link," *Radio Engineering*, vol. 19, no. 2, pp. 271-277, 2010.

[43] H. S. Saini, R. K. Singh, and K. S. Reddy, *Innovations in Electronics and Communication Engineering*, Springer Science and Business Media LLC, 2020.

[44] Q. V. Minh, N. T. Nguyen, H. T. Pham, and N. T. Dang, "Performance enhancement of LEO-to-ground FSO systems using all-optical HAP-based relaying," *Physical Communication*, vol. 31, pp. 218-229, 2018.

[45] J. Jignesh, U. Sripati, and M. Kulkarni, "Performance of QPSK modulation for FSO geo-synchronous satellite communication link under atmospheric turbulence," in *Proc. International Conference on Microelectronics, Communication and Renewable Energy*, 2013.

[46] Y. Ata and Y. Baykal, "Effect of anisotropy on bit error rate for an asymmetrical Gaussian beam in a turbulent ocean," *Applied Optics*, vol. 57, no. 9, pp. 2258-2262, 2018.

[47] M. Ijaz, Z. Ghassemlooy, J. Perez, V. Brazda, and O. Fiser, "Enhancing the atmospheric visibility and fog attenuation using a controlled FSO channel," *IEEE Photonics Technology Letters*, vol. 25, no. 13, pp. 1262-1265, 2013.

[48] H. Kasban, "Detection of buried objects using acoustic waves," M. Sc. thesis, Faculty of Electronic Engineering, Egypt, 2008.

[49] M. Baskaran, S. Ethiraj, and T. Gokulakrishnan, "Eliminating the effects of fog and rain attenuation for live video streaming on free space optics," *International Journal of Systems, Algorithms & Applications*, vol. 2, 2012.

[50] H. Kasban and M. A. M. El-Bendary, "Performance improvement of digital image transmission over mobile WiMAX networks," *Wireless Personal Communications*, vol. 94, pp. 1087–1103, 2017.

Adel Zaghloul Mahmoud received B.Sc. degree in Electronic and Electrical Communication Engineering from El-Mansoura University, M.Sc. degree in Electronic and Electrical Communication Engineering from El-Azhar University, and PH.D. degree in Electronic and Electrical Communication Engineering from El Menufia University, Egypt. He is Associate Professor in Faculty of Engineering, Zagazig University, Egypt. He was born in Sinblaween, Dakhlih Governorate, Egypt, in 1960. His research areas of interest are in, optical waveguides, electrooptic devices, optical fibers, free space optics.

AbdelHamid Shalaan received B.Sc., M.Sc. and PH.D. degrees in Electrical and Electronic Engineering from Menoufia University, Egypt. Currently, He is the Head of Electronics and Communications Department, faculty of Engineering, Zagazig University, Egypt. He was born in Menouf, Menoufia Governorate, Egypt, in 1959. His research areas of interest are in, optical waveguides, free space optics, antennas and waves propagation.

Hani Kasban received B.Sc., M.Sc. and PH.D. degrees in Electrical and Electronic Engineering from Menoufia University, Egypt. Currently, He is the Head of Engineering and Scientific Instruments Department, Nuclear Research Center (NRC), Egyptian Atomic Energy Authority (EAEA), Cairo, Egypt. He is a co-author of international journals papers.

His research areas of interest are in, electronics, digital signal processing, communication systems and nuclear applications in industry and medicine.

Amaal Ashraf received B.Sc., from Electrical Engineering Department, Higher of Technological Institute (HTI), 10th of Ramadan City, Egypt in 2008 and M.Sc. degree from the Electronics and Communications Engineering Department, Zagazig, Egypt, in 2014. She is currently an Assistant Lecture with the Electronic and Communication Engineering Department, Higher of Technological Institute, 10th of Ramadan City, Egypt.